Determination of refractive indices of porcine skin tissues and Intralipid at eight wavelengths between 325 and 1557 nm

Huafeng Ding, Jun Q. Lu, Kenneth M. Jacobs, and Xin-Hua Hu

Department of Physics, East Carolina University, Greenville, North Carolina 27858

We constructed an automated reflectometry system for accurate measurement of coherent reflectance curves of turbid samples and analyzed the presence of coherent and diffuse reflection near the specular reflection angle. An existing method has been validated to determine the complex refractive indices of turbid samples on the basis of nonlinear regression of the coherent reflectance curves by Fresnel's equations. The complex refractive indices of fresh porcine skin epidermis and dermis tissues and Intralipid solutions were determined at eight wavelengths: 325, 442, 532, 633, 850, 1064, 1310, and 1557 nm. © 2005 Optical Society of America

OCIS codes: 170.6930, 290.3030, 170.7050.

1. INTRODUCTION

Boundaries of a homogeneous biological tissue or interfaces within a heterogeneous tissue play a unique role in our understanding of tissue optics. On one hand, light distribution within a tissue for a given configuration of source has to be solved in terms of specific boundary problems, and thus appropriate boundary conditions are required. On the other hand, detection of light signals external to the tissue invariably involves light transportation through the tissue boundary, and the effect of the boundary needs to be accounted for to determine optical parameters accurately. In the cases where light scattering is negligible, light interaction with interfaces can be clearly understood in terms of refractive-index mismatch on the basis of the theory of electrodynamics. For most biological tissues, however, light scattering dominates from ultraviolet to near-infrared spectral regions, and the concept of refractive index requires careful deliberation. To our knowledge, no satisfactory results have been reported on a theoretical framework for refractive indices of biological tissues that are homogeneous on macroscopic scales of millimeter or larger. It is likely, however, that some forms of effective-medium theory developed for simple turbid systems of two or a few compositions, such as sphere suspensions, may be extended to biological tissues. On the basis of the effective-medium theory, the coherent component of light reflected from or transmitted though a turbid sample of sphere suspension can be measured to determine the refractive index of the medium.[1] Limited studies have shown that refractive index can be used in modeling of tissue optics to characterize the effect of sample interfaces with ambient media on the inverse determination of bulk parameters and light distribution in heterogeneous tissues.[2–4] It is therefore an important task to obtain accurately the refractive index of tissues and its variation with wavelength for further improving tissue optics modeling, image reconstruction,[5] and instrumentation development.

The challenge to determine accurately the refractive index of biological tissues from reflectance or transmittance measurements is significant because of the presence of strong scattering. Measurements of specular reflectance at one or a few angles of incidence have been employed to determine complex refractive index for absorbing samples[6–8] and turbid and biological samples.[9,10] Other reported methods include distribution measurement of light transmitted through an optical fiber with a tissue as the fiber cladding[11] and of coherent reflection inside a tissue by using optical coherence tomography systems with a converging light beam.[12–14]

To determine the refractive index of biological tissues, we have constructed an automated reflectometry system to measure accurately a coherent reflectance curve $R(\theta)$, i.e., the coherent reflectance R of a turbid sample interfacing with a glass prism as a function of incident angle θ. In comparison with other methods, our approach requires no measurement of tissue thickness and minimal processing of tissue samples to maintain their structural integrity. Furthermore, the automated system makes possible the measurement of reflectance curves over a large range of incident angle and thus improves the accuracy of refractive-index determination for turbid samples with no total reflection.

In this paper we describe the design of the reflectometer system and the validation of the method by comparing contributions to $R(\theta)$ by diffusely reflected light among turbid samples with deionized water as the baseline. The complex refractive index of a sample is determined by a nonlinear regression of $R(\theta)$ with the Fresnel equations, and results are presented for complex refractive indices of 20% Intralipid solutions and fresh porcine skin epidermis and dermis at eight wavelengths between 325 and 1557 nm.

2. METHODS

The method of measuring the critical angle of total reflection has long been used to determine the refractive index of liquid and other samples interfacing with a high-index

1084-7529/05/061151-7/$15.00

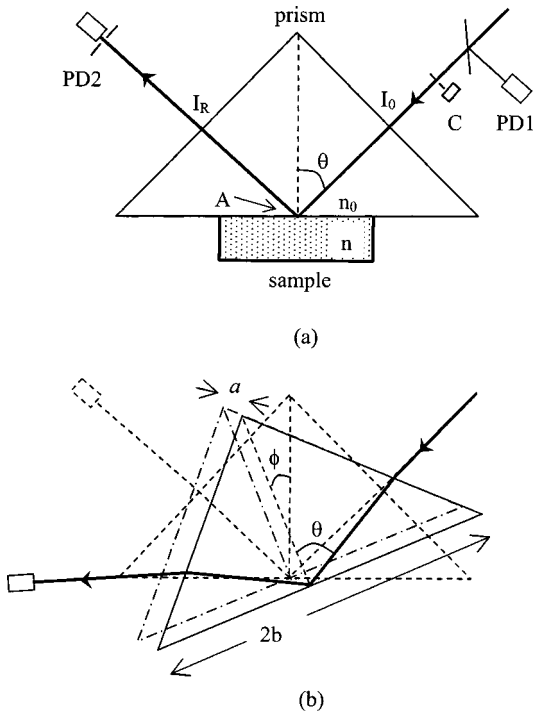

Fig. 1. Schematic of the reflectometry system: (a) the aligned position with $\theta=45°$; PD1/PD2, photodiodes; C, chopper; (b) the varied position of the prism and sample by rotation from the aligned positions (dashed lines) through ϕ (dashed–dotted lines) and translation over distance a (solid lines).

glass prism and has been extended to absorbing and turbid samples by measuring the coherent reflectance curve $R(\theta)$.[9,10] We adopted this approach to measure the coherent reflectance R of a tissue or Intralipid sample as a function of incident angle θ from the interface between the sample and a glass prism. The measured $R(\theta)$ were fitted with the calculated values of coherent reflectance from Fresnel's equations, which requires the assumed value of the complex refractive index of the sample $n=n_r+in_i$ and the known refractive index n_0 of the prism. The value of n was inversely determined by using an iteration process to achieve the least-squares difference between the measured and the calculated R.

The above approach has been realized for this study with an automated system that was designed to provide four degrees of freedom to rotate and translate a sample in contact with the base surface of a 30–42–30-cm right-angle prism of BK7 glass and with a photodiode detector for the measurement of $R(\theta)$. A schematic of the optical setup is shown in Fig. 1. A collimated laser beam of power I_0 was incident on one side of the prism, which was rotated and translated by two stepping motors so that the laser beam coincided with the center of the prism base at an incident angle θ. The reflected beam propagating along the specular reflection angle exited symmetrically from the other side surface of the prism, and its power I_R was measured with another photodiode PD2. PD2 was rotated and translated by two stepping motors so that the sensor surface was centered and aligned perpendicular to the reflected beam for each value of θ. The prism was first aligned at $\theta=45°$ with the incident beam transmitted straight through the entrance side, as shown in Fig. 1(a). To adjust the incident angle θ to another value larger than 45°, the prism was rotated through an angle ϕ around its base center A, satisfying

$$\sin\phi = n_0 \sin(\theta - 45°), \tag{1}$$

and then translated over a distance a given by

$$a = b\left[\frac{\sin(90° - \theta)}{\sin(45° + \theta)} - \frac{\sin(45° - \phi)}{\sin(90° + \phi)}\right], \tag{2}$$

where $2b=42.43$ mm is the length of the prism base, as shown in Fig. 1(b). PD2 was rotated and translated according to similar formulas to measure I_R.

The incident beams, modulated at 370 Hz with a mechanical chopper, were provided by one of seven cw lasers generating radiation at eight wavelengths of 325, 442, 532, 633, 850, 1064, 1310, and 1557 nm, with I_0 adjusted to be near 1 μW. The incident beam was linearly polarized in either s or p orientation with a Glan–Thompson polarizer. Two Si or GaAs photodiodes were used to measure I_0 and I_R with a pinhole of 2-mm diameter in front of the photodiode on the reflection side of the prism to reduce any contribution of diffuse reflection to I_R. The control of the four stepping motors and acquisition of I_R data with a lock-in amplifier and I_0 data with an analog-to-digital board were accomplished with in-house developed software through a personal computer. Angle θ was varied between 48° and 80° with a step of 0.125° and resolution of 0.006°, and the rotation angles and translation distances of the prism and photodiode were tabulated for each value of θ. The coherent reflectance curves $R(\theta)$ were measured with either an s- or a p-polarized incident beam to investigate the correlation among refractive indices of porcine skin samples

$$R_s(\theta) = C_s(\theta) I_R(s,\theta)/I_0, \tag{3}$$

and

$$R_p(\theta) = C_p(\theta) I_R(p,\theta)/I_0, \tag{4}$$

where C_s and C_p are scaling factors that can be calculated at each angle θ from the refraction of the incident and reflected beams with s (p) polarization, respectively, at the side surfaces of the glass prism and from light attenuation within the prism.

We determined the complex refractive indices of fresh porcine skin tissues. The skin samples, of medium complexion, were obtained from the dorsal neck area of white domestic 6-month-old pigs at the Brody School of Medicine, East Carolina University. The skin patches were stored in a bucket on crushed ice (~2 °C) inside a refrigerator immediately after removal from the pig. The samples, of approximately 1×1 cm^2, were prepared by removing the hair on the skin surface with scissors and excising subcutaneous fat tissue with a razor blade. They were warmed to room temperature (20±2 °C) with 0.9% saline drops. Each skin sample was pressed against the base of the prism with a piston pressurized by a nitrogen gas cylinder to maintain good contact between the sample and the prism. The periphery of the tissue sample between the piston and the prism base was sealed with plastic tape to prevent sample dehydration. By pressing either the epidermis or the dermis side of the skin sample

against the prism base, the respective indices were determined. Histologic examination of the vertical sections of the porcine skin revealed that the stratum corneum layer of the epidermis has a typical thickness of 10-μm in comparison with the total epidermis of ~100 μm. On the basis of previous study of the ultraviolet light penetration through epidermis of Caucasian skin with similar structures,[15] we expect optical penetration through the full epidermis at all the wavelengths reported here. Therefore the refractive index obtained by pressing the epidermis side of a skin sample against the prism should be regarded as the averaged value over the epidermis including the top layer of stratum corneum. To compare the skin data with a widely used tissue phantom medium, we also determined the refractive index of Intralipid solution samples at different concentrations by volumetrically diluting the Intralipid solution of 20% concentration by weight (Fresenius Kabi Clayton, L. P.) with deionized water. The liquid sample was in contact with the prism base within a sample holder centered at the prism base. All reflectance measurements were performed at room temperature within 30 h of animal euthanasia.

The complex index of refraction of a sample $n=n_r+in_i$ at each wavelength was solved with a method of least squares based on the Marquardt–Levenberg nonlinear regression algorithm[16] by fitting the calculated values, $\tilde{R}_s(\theta)$ and $\tilde{R}_p(\theta)$, to the measured values, $R_s(\theta)$ and $R_p(\theta)$, respectively, by using the known n_0 of the prism. The calculated coherent reflectances at the prism–sample interface are given by the well-known Fresnel's equations as[17]

$$\tilde{R}_s(\theta)=\left|\frac{n_0\cos\theta-[(n_r+in_i)^2-{n_0}^2\sin^2\theta]^{1/2}}{n_0\cos\theta+[(n_r+in_i)^2-{n_0}^2\sin^2\theta]^{1/2}}\right|^2, \quad (5)$$

$$\tilde{R}_p(\theta)=\left|\frac{(n_r+in_i)^2\cos\theta-n_0[(n_r+in_i)^2-{n_0}^2\sin^2\theta]^{1/2}}{(n_r+in_i)^2\cos\theta+n_0[(n_r+in_i)^2-{n_0}^2\sin^2\theta]^{1/2}}\right|^2. \quad (6)$$

The consistency between the measured and the calculated coherent reflectance curves is described by a coefficient of determination, R^2, ranging between 0 and 1 and is defined as

$$R^2=1-\frac{\sum_{j=1}^{N}(R_j-\tilde{R}_j)^2}{\sum_{j=1}^{N}(R_j-\bar{R})^2}, \quad (7)$$

where R_j and $\tilde{R}_j$ denote the measured and the calculated reflectance at the ith angle of incidence θ_j, respectively, and $\bar{R}$ is the mean value of measured reflectance over N values of θ. A perfect fit would yield $R^2=1$. The parameter R^2 is larger than 0.990 for water and Intralipid samples and ranges from 0.970 to 0.999 for skin dermis samples and from 0.950 to 0.999 for epidermis. The system was calibrated before measurement of each sample by determining the refractive index of deionized water and comparing it with the published value at the wavelength of measurement.[18] The nonlinear regression of the measured coherent reflectance based on Fresnel's equations exhibited different sensitivities to the variations of n_r and n_i. For water and Intralipid samples of low concentrations, the existence of the critical angle of total reflection restricts the choice of n_r with a sensitivity of 0.002 or less. In these cases the regression was insensitive to the values of n_i as long as $n_i<5\times10^{-4}$. For samples of strong turbidity, the disappearance of the critical angle and deviation from Fresnel's equations in the case of tissues causes degraded sensitivity of 0.004 for n_r and a sensitivity of 0.002 for the increased n_i. The total uncertainty in n of the sample was estimated to be $\Delta n_r=\pm0.002$ and $\Delta n_i=\pm0.001$ for Intralipid and $\Delta n_r=\pm0.004$ and $\Delta n_i=\pm0.002$ for the porcine skin tissues.

3. RESULTS

The coherent reflectance curves $R(\theta)$ of deionized water have been measured for calibration of the system and provide the baseline data for investigations of the diffuse-reflection contribution to $R(\theta)$. Typical results of $R_s(\theta)$ and $R_p(\theta)$ measurements with a sample of deionized water at 633 nm are shown in Fig. 2 with R^2 about ~0.999. The real refractive index n_r was determined from the fitting as 1.332 and 1.333 for s and p polarization, respectively, and the imaginary index n_i was less than 5×10^{-4}, the lower limit of this method. These measurements were repeated at the other seven wavelengths, and the values of n_r agreed well with the published values within the experimental error.[18] We also determined whether the reflected light signal measured with the photodiode (PD2 in Fig. 1) and aperture would correctly yield coherent reflectance for the turbid samples of Intralipid and skin dermis. For this purpose, the collimated beam of $\lambda=633$ nm was used to measure the distribution of light reflected from the interface between the sample and the prism at either $\theta=45°$ or 70° by rotating the photodiode PD2 about the center of the prism base. The reflected light signal was measured between −4° and 4° of the rotation angle of PD2 and is plotted in Fig. 3. These results demonstrate that the amount of coherently reflected light is much larger than that of diffusely reflected light, even for skin tissue samples.

For Intralipid samples, the complex refractive indices were determined as a function of both concentration and wavelength. The measurements of $R_s(\theta)$ and $R_p(\theta)$ were

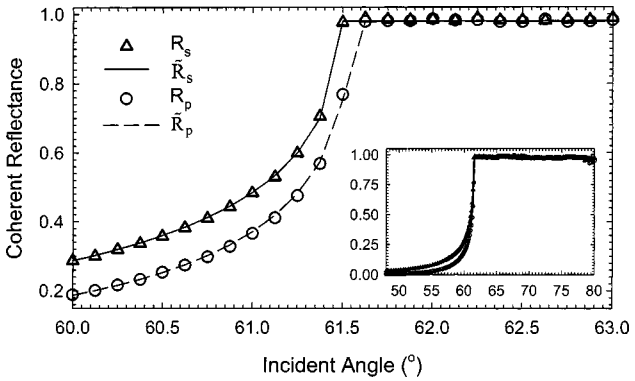

Fig. 2. Measured (R_s and R_p) and calculated ($\tilde{R}_s$ and $\tilde{R}_p$) coherent reflectance versus incident angle for deionized water with s- and p-polarized incident beam at $\lambda=633$ nm. Inset, full angular range.

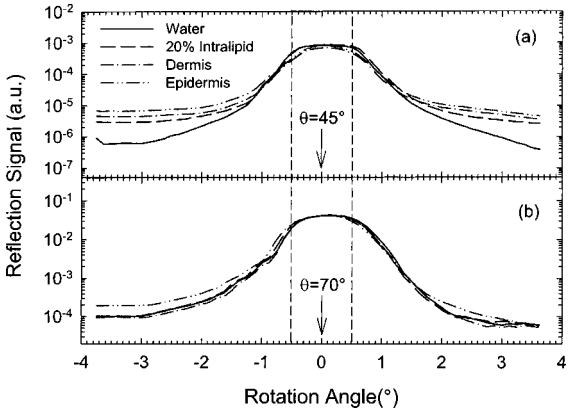

Fig. 3. Reflection signal versus rotation angle of the detector at incident angle of (a) $\theta=45°$, (b) $\theta=70°$ with an s-polarized beam at $\lambda=633$ nm for deionized water, 20% Intralipid solution, and porcine skin epidermis and dermis with an angular step of 0.125°. Error bars of approximately ±5% have been removed for clarity; the two vertical dashed lines indicate the angular acceptance range of the aperture in front of the photodiode.

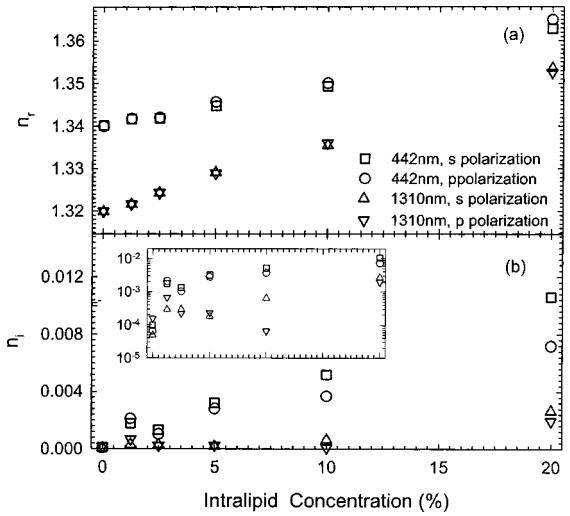

Fig. 4. Refractive indices of Intralipid samples versus concentration by weight: (a) real; (b) imaginary; inset, with the log scale.

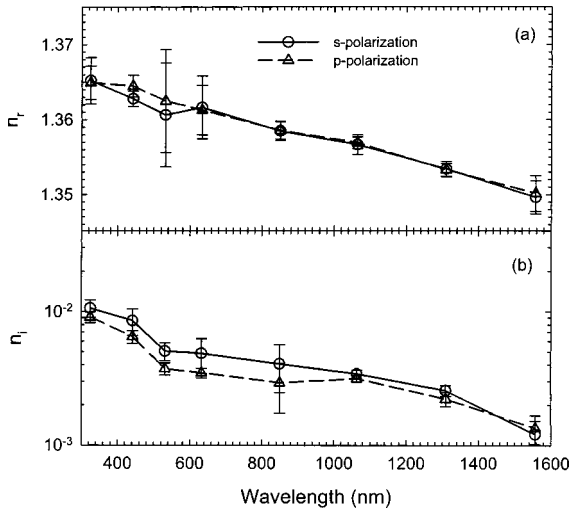

Fig. 5. (a) Real and (b) imaginary refractive indices of 20% Intralipid versus wavelength. The symbols and error bars are the mean values and standard deviations of five values of the refractive index, and the curves are provided as visual aids.

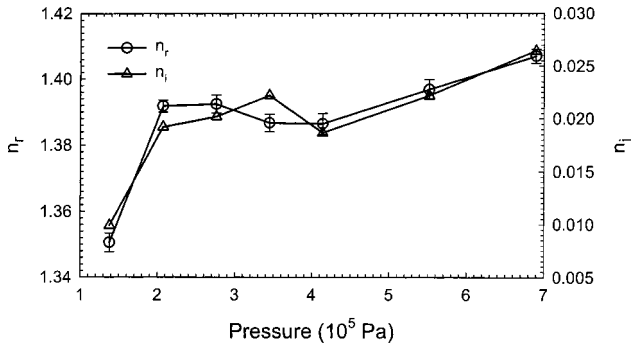

Fig. 6. Real and imaginary indices of refraction of porcine skin dermis versus sample pressure. The symbols and error bars are the mean values and standard deviations of three values of the refractive index.

performed twice for each sample to obtain the mean values of complex refractive indices by nonlinear regression of each coherent reflectance curve at different Intralipid concentrations and wavelengths. The agreement between the measured values of $R_s(\theta)$ and $R_p(\theta)$ and the calculated ones from Fresnel's Eqs. (5) and (6) was excellent, with R^2 above 0.990 and thus very close to that of deionized water. The concentration dependence of the mean value of real refractive index at all eight wavelengths was found to be linear, and two examples, at $\lambda=442$ and 1310 nm, are shown in Fig. 4. For wavelengths larger than 600 nm, the imaginary refractive indices were less than the accuracy afforded by the reflectometry system, 1×10^{-3} and thus appear fluctuating. For short wavelengths, such as 442 nm, the imaginary indices of samples of high concentration at 5%, 10%, and 20% are sufficiently large and reveal a concentration dependence close to linear. For Intralipid samples of 20% concentration, we carried out three additional measurements to obtain individual values of complex refractive index. These were combined with the previous results to obtain the mean values and standard deviations of the index as functions of wavelength, which are represented as the symbols and error bars in Fig. 5.

Because a piston pressurized by a nitrogen gas cylinder was used to maintain good contact between tissue and prism, the effect of the pressure on the index determination needed to be evaluated. The dependence of the real refractive index of the porcine skin dermis on pressure was obtained with three measurements of reflectance curves from two skin samples, and the results are shown in Fig. 6. It can be seen from the data that the real index is not sensitive to air pressure between 2×10^5 and 5×10^5 Pa, and all subsequent measurements of coherent reflectance of skin tissue samples were carried out at a fixed pressure of 2.06×10^5 Pa (30 psi or 2.0 atm) to avoid possible damage to tissue structure due to excessive pressure. At each of the eight wavelengths, three skin samples from different pigs were used to measure the coherent reflectance curves $R_s(\theta)$ and $R_p(\theta)$, and the measurements

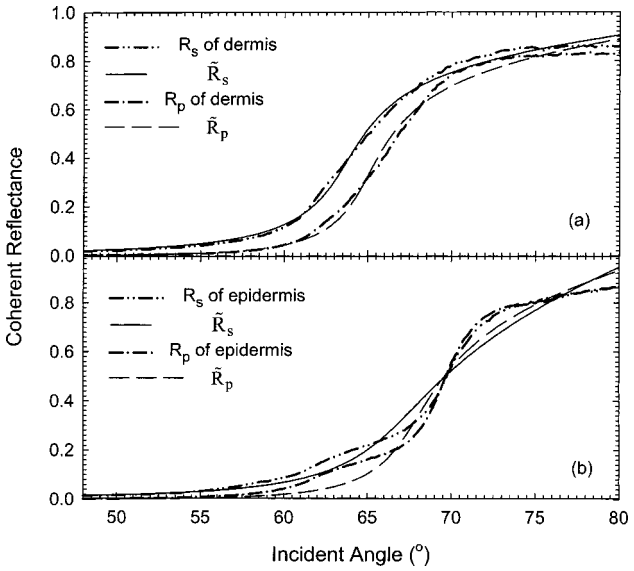

Fig. 7. Measured (R_s and R_p) and calculated ($\tilde{R}_s$ and $\tilde{R}_p$) coherent reflectance versus incident angle at $\lambda = 1064$ nm from one sample: (a) dermis with $R^2 = 0.997$ for s and 0.994 for p polarization, (b) epidermis with $R^2 = 0.981$ for both s and p polarization.

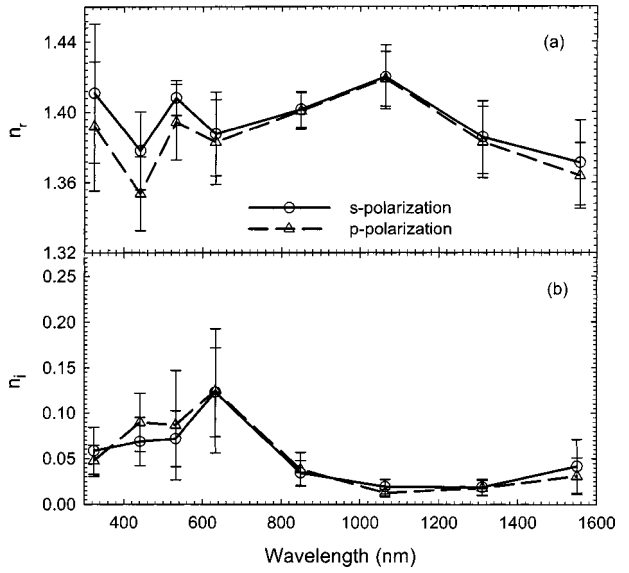

Fig. 8. (a) Real and (b) imaginary refractive indices of porcine skin epidermis versus wavelength. The symbols and error bars are the mean values and standard deviations of nine values of the refractive index, and the curves are provided as visual aids.

were performed three times for each sample. Typical results of $R_s(\theta)$ and $R_p(\theta)$ are shown in Fig. 7 for the dermis and epidermis of a skin sample. Nonlinear regressions of $R_s(\theta)$ and $R_p(\theta)$ data by Fresnel's equations were done individually on each measured reflectance curve, and they were worse than the cases of water and Intralipid samples, with R^2 ranging between 0.920 and 0.999. The mean values and standard deviations of the nine values of the index for each combination of wavelength and polarization are plotted as the symbols and error bars in Fig. 8 for the porcine skin epidermis and in Fig. 9 for the dermis.

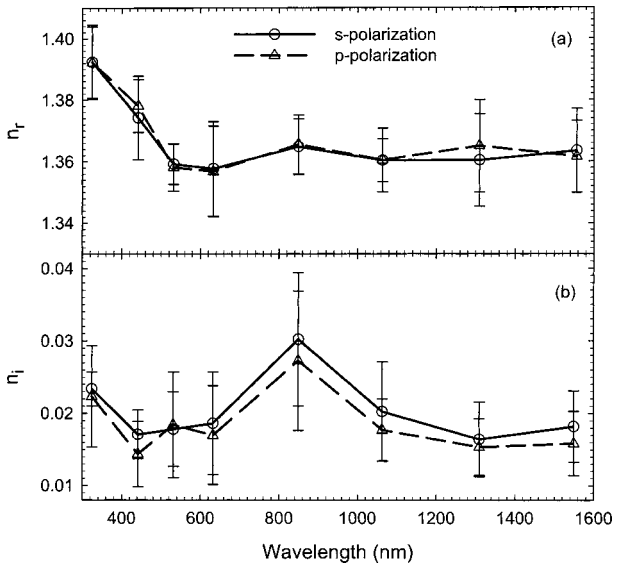

Fig. 9. (a) Real and (b) imaginary refractive index of porcine skin dermis versus wavelength. The symbols and error bars are defined as in Fig. 8, and the curves are provided as visual aids.

4. DISCUSSION

Index of refraction is an important parameter of tissue optics. This is manifested by the recent investigations of surface effect on inverse determination of bulk parameters of turbid samples.[2,4] Moreover, comprehension of index-mismatched interfaces may play a critical role in quantitative modeling of imaging data and in developing *in vivo* image-based methods for inverse determination of tissue optical parameters. To solve the challenging problem of determining refractive index, we have constructed an automated reflectometry system that enabled us to accurately measure coherent reflectance curves of turbid samples. Combined with nonlinear regression analysis based on Fresnel's equations, this method provides a robust approach to determining *in vitro* the complex refractive index of skin tissues with minimal tissue processing. In comparison with the coherent-transmittance-based approach,[19] coherent reflectance signals do not depend on sample thickness as long as it is much greater than the light wavelength, and the signals become large at large θ even for samples with high attenuation coefficients. This feature is especially important for soft tissue samples because large uncertainty exists in the thickness measurements owing to the deformable sample shapes.

The validity of the coherent-reflectance-curve method depends in part on the dominance of coherent over diffuse reflection at the specular reflection angle. The diffuse reflection originates from two sources: rough interfaces with mismatched indices and bulk scattering. It has been shown that the interface between the glass of the prism and the turbid sample plays an important role in distribution of light signals external to a turbid sample even for a modest index mismatch of 0.1.[4] Using two types of turbid samples of 20% Intralipid and porcine skin tissues, one can compare the effects of these two sources. We first verified that a well-defined, coherently reflected beam exists even for the highly turbid sample of 20% Intralipid and for skin tissues of layered structure. The skin dermis

samples exhibit angular distribution of reflection signal near the specular reflection angle similar to that of the Intralipid, as shown in Fig. 3. Therefore the skin dermis samples are expected to have very good contact with the prism glass, and thus the effect of surface roughness is negligible on reflection signals within an angular range of 1° from the specular angle. The epidermis sample, on the other hand, presents significant diffuse reflection outside the angular range of 1° for both angles of incidence of 45° and 70°. For the reflected light signals measured by the photodiode with an aperture, shown in Fig. 3 with two vertical dashed lines, it is clear that contribution by diffusely reflected light decreases significantly as θ increases toward 90° for all three types of samples. The diffuse reflection likely affected the determination of epidermis index most among the three types of samples and can be related to the condition of the sample surface and its layered structure by comparison with the data of dermis, as discussed below.

The consistency of the measured and the calculated coherence reflectance curves is described by the value of coefficient of determination R^2, defined by Eq. (7). Among a total of ~140 measurements of the porcine skin dermis samples, a majority of 94% have R^2 larger than 0.990, with only 6% between 0.97 and 0.99. In contrast, more than half (57%) of the 140 measurements for porcine skin epidermis have R^2 ranging from 0.97 to 0.99, with 28% larger than 0.990 and 15% between 0.95 and 0.97. This difference may be attributed to the different surface conditions of the skin samples and the marked difference in tissue heterogeneity between the skin epidermis and dermis. The surface of a fresh porcine skin sample after hair cleaning with scissors, is a horny layer of stratum corneum with dead keratinocytes and embedded hairs and thus is harder and less homogeneous than the dermis side of the prepared skin samples. Moreover, the layered structure of the epidermis presents considerably greater tissue heterogeneity than the relatively homogeneous, bloodless dermis for *in vitro* skin samples. Even under a pressure of 2.06×10^5 Pa to achieve good contact with the prism, the epidermis–prism interface is expected to have a significant degree of roughness that causes a higher contribution of diffuse reflection to $R(\theta)$ than that of the deep, soft, reticular dermis side of porcine skin samples. This is consistent with the data presented in Fig. 3, which show that diffuse reflection from the epidermis sample is strongest among the three types of samples, and with the fact that the imaginary refractive index of epidermis samples is larger than that of the dermis, as shown in Figs. 8(b) and 9(b). It is for these reasons that coherent reflectance needs to be measured at a large range of incident angles, especially those over 65°, to minimize the surface effect on the real refractive index determined through nonlinear regression. In this sense, our automated reflectometry system has a clear advantage over the previous methods that measured $R(\theta)$ at only a few angles.[6,7,9,10]

We calculated the correlation coefficients r_{corr} of the wavelength dependence of the refractive index between the values determined with an *s*-polarized and a *p*-polarized beam and found r_{corr} to be 0.82 for the skin epidermis and 0.96 for dermis samples. Since different skin samples from different pigs were used for this study over a period of one year, the high values of r_{corr} demonstrate that the coherent-reflectance-curve method that we have validated in this report provides a reliable method to determine refractive index of biological tissue samples. In contrast, the refractive indices of epidermis and dermis samples exhibit different wavelength dependence, and r_{corr} was found to be close to zero with $r_{corr}=0.023$ between epidermis and dermis samples with the *s*-polarized beam and $r_{corr}=0.043$ with the *p*-polarized beam. These results clearly indicate that the skin epidermis and dermis should be treated as two types of tissues having different optical properties for accurate modeling. The wavelength dependence of the real refractive index n_r has not previously been reported for either human or porcine skin tissues. Within experimental error our *in vitro* results on the n_r of porcine skin epidermis and dermis at $\lambda=1310$ nm agree with those determined *in vivo* from human skin tissues by optical coherence tomography for epidermis.[13] The n_r of dermis, however, is smaller than those determined by optical coherence tomography.[12,13] The wavelength dependence of the n_r of dermis is similar to that of bovine and porcine muscle tissues in the visible region.[10,11]

Modeling of electromagnetic wave propagation in turbid media with scatterer sizes on the same scale as the wavelength remains a challenge. Attempts have been made to apply an effective-medium theory to understand the coherent reflection by a system of uniform spheres. In such a theory an effective index of refraction n_{eff} can be expressed as a function of the scattering matrix elements of a single sphere.[1] In the limit of low concentration, the imaginary part of n_{eff} has been shown to be linearly related to the sphere or scatterer concentration, as proposed earlier by van de Hulst with a simpler approach.[20] For turbid samples with complex distribution of scatterer size, scatterer shape, and structural heterogeneity, such as Intralipid and skin tissues, however, modeling of the complex refractive index is still an open question. This is especially the case when the interface between the prism and the tissue sample cannot be assumed optically smooth, as we have demonstrated with our results from epidermis and dermis samples. For these reasons we would like to point out that the use of coherent reflectance curves may not provide a reliable method to determine the ultraviolet absorption coefficient of a tissue sample, even for corneal tissues that are clear to visible light.[8] To achieve this goal, it is required that (1) the effect of surface roughness be eliminated by good matching of index or be accurately modeled, and (2) that the relation between imaginary refractive index and absorption and scattering coefficient be determined.

ACKNOWLEDGMENTS

The authors thank Yousu Sun and Dale Aycock for providing fresh porcine skin samples for this study. JQL acknowledges partial support by National Institutes of Health grant (1R15GM70798-01).

Comments and correspondence should be sent to X. H. Hu at hux@mail.ecu.edu.

REFERENCES

1. R. G. Barrera and A. Garcia-Valenzuela, "Coherent reflectance in a system of random Mie scatterers and its relation to the effective-medium approach," J. Opt. Soc. Am. A **20**, 296–311 (2003).
2. M. A. Bartlett and H. Jiang, "Effect of refractive index on the measurement of optical properties in turbid media," Appl. Opt. **40**, 1735–1741 (2001).
3. T. J. Farrell and M. S. Patterson, "Experimental verification of the effect of refractive index mismatch on the light fluence in a turbid medium," J. Biomed. Opt. **6**, 468–473 (2001).
4. X. Ma, J. Q. Lu, and X. H. Hu, "Effect of surface roughness on determination of bulk tissue optical parameters," Opt. Lett. **28**, 2204–2206 (2003).
5. A. Godavarty, D. J. Hawrysz, R. Roy, and E. M. Sevick-Muraca, "Influence of the refractive index-mismatch at the boundaries measured in fluorescence enhanced frequency-domain photon migration imaging," Opt. Express **10**, 653–662 (2002).
6. J. Fahrenfort and W. M. Visser, "On the determination of optical constants in the infrared by attenuated total reflection," Spectrochim. Acta **18**, 1103–1116 (1962).
7. W. Leupacher and A. Penzkofer, "Refractive-index measurement of absorbing condensed media," Appl. Opt. **23**, 1554–1558 (1984).
8. G. H. Pettit and M. N. Ediger, "Corneal-tissue absorption coefficients for 193- and 213-nm ultraviolet radiation," Appl. Opt. **35**, 3386–3391 (1996).
9. G. H. Meeten and A. N. North, "Refractive index measurement of absorbing and turbid fluids by reflection near the critical angle," Meas. Sci. Technol. **6**, 214–221 (1995).
10. H. Li and S. Xie, "Measurement method of the refractive index of biotissue by total internal reflection," Appl. Opt. **35**, 1793–1795 (1996).
11. F. P. Bolin, L. E. Preuss, R. C. Taylor, and R. J. Ference, "Refractive index of some mammalian tissues using a fiber optic cladding method," Appl. Opt. **28**, 2297–2303 (1989).
12. G. J. Tearney, M. E. Brezinski, J. F. Southern, B. E. Bouma, M. R. Hee, and J. G. Fujimoto, "Determination of the refractive index of highly scattering human tissue by optical coherence tomography," Opt. Lett. **20**, 2258–2260 (1995).
13. A. Knüttel and M. Boehlau-Godau, "Spatially confined and temporally resolved refractive index and scattering evaluation in human skin performed with optical coherence tomography," J. Biomed. Opt. **5**, 83–92 (2000).
14. X. Wang, C. Zhang, L. Zhang, L. Xue, and J. Tian, "Simultaneous refractive index and thickness measurements of bio tissue by optical coherence tomography," J. Biomed. Opt. **7**, 628–632 (2002).
15. M. A. Everett, E. Yeargers, R. M. Sayre, and R. L. Olson, "Penetration of epidermis by ultraviolet rays," Photochem. Photobiol. **5**, 533–542 (1966).
16. D. W. Marquardt, "An algorithm for least squares estimation of parameters," SIAM (Soc. Ind. Appl. Math.) J. Numer. Anal. **11**, 431–441 (1963).
17. J. D. Jackson, *Classical Electrodynamics*, 3rd ed. (Wiley, New York, 1999).
18. G. Hale and M. Querry, "Optical constants of water in the 200 nm to 200 micrometer wavelength region," Appl. Opt. **12**, 555–563 (1973).
19. J. H. Page, P. Sheng, H. P. Schriemer, I. Jones, X. D. Jing, and D. A. Weitz, "Group velocity in strongly scattering media," Science **271**, 634–637 (1996).
20. H. C. van de Hulst, *Light Scattering by Small Particles* (Wiley, New York, 1957).